The observed non-equivalence (by 7σ) between the two terminal N3—C lengths in (5) is unexpected and not readily explicable. It is tempting to speculate that this implies differences in reactivity and to the oxidative metabolism of triazenes that occurs at just one of these two methyl groups. The crystal structures of further dimethyltriazenes should serve to illuminate this issue.

This work was supported by grants from the Cancer Research Campaign.

References

BONADONNA, G., USLENGHI, C. & ZUCALI, R. (1975). *Eur. J. Cancer*, pp. 251–266.

BREITHAUPT, H., DAMMANN, A. & AIGNER, K. (1982). *Cancer Chemother. Pharmacol.* **9**, 103–109.

CONNORS, T. A., GODDARD, P. M., MERAI, K., ROSS, W. C. J. & WILMAN, D. E. V. (1976). *Biochem. Pharmacol.* **25**, 241–246.

EDWARDS, S. L., CHAPUIS, G., TEMPLETON, D. H. & ZALKIN, A. (1977). *Acta Cryst.* B**33**, 276–278.

EDWARDS, S. L., SHERFINSKI, J. S. & MARSH, R. E. (1974). *J. Am. Chem. Soc.* **96**, 2593–2597.

ELKS, J. & HEY, D. H. (1943). *J. Chem. Soc.* pp. 441–445.

FRENZ, B. A. (1981). *Enraf–Nonius Structure Determination Package*. Enraf–Nonius, Delft, The Netherlands.

FRONCZEK, F. R., HANSCH, C. & WATKINS, S. F. (1988). *Acta Cryst.* C**44**, 1651–1653.

GESCHER, A., HICKMAN, J. A., SIMMONDS, R. J., STEVENS, M. F. G. & VAUGHAN, K. (1978). *Tetrahedron Lett.* **50**, 5041–5044.

GUIMANINI, A. G., LASSIANI, L., NISI, C., PETRIC, A. & STANOVNIK, B. (1983). *Bull. Chem. Soc. Jpn*, **56**, 1887–1898.

KURODA, R. & WILMAN, D. E. V. (1985). *Acta Cryst.* C**41**, 1543–1545.

MAIN, P., FISKE, S. J., HULL, S. E., LESSINGER, L., GERMAIN, G., DECLERCQ, J.-P. & WOOLFSON, M. M. (1982). *MULTAN*11/82. *A System of Computer Programs for the Automatic Solution of Crystal Structures from X-ray Diffraction Data*. Univs. of York, England, and Louvain, Belgium.

MILES, D. W. & SOUHAMI, R. L. (1987). *Bailliere's Clin. Oncol.* **1**, 551–573.

NEIDLE, S., WEBSTER, G. D., KURODA, R. & WILMAN, D. E. V. (1987). *Acta Cryst.* C**43**, 674–676.

RAMOS, M. N. & PEREIA, S. R. (1986). *J. Chem. Soc. Perkin Trans.* 2, pp. 131–133.

RANDALL, A. J., SCHWALBE, C. H. & VAUGHAN, K. (1984). *J. Chem. Soc. Perkin Trans.* 2, pp. 251–253.

VAUGHAN, K., TANG, Y., LLANOS, G., HORTON, J. K., SIMMONDS, R. J., HICKMAN, J. A. & STEVENS, M. F. G. (1984). *J. Med. Chem.* **27**, 357–363.

WALKER, N. & STUART, D. (1983). *Acta Cryst.* A**39**, 158–166.

WILMAN, D. E. V. (1985). *Biological Oxidation of Nitrogen in Organic Molecules. Chemistry, Toxicology and Pharmacology*, edited by J. W. GORROD & L. A. DAMANI, pp. 297–302. Chichester: Ellis Horwood.

WILMAN, D. E. V., COX, P. J., GODDARD, P. M., HART, L. I., MERAI, K. & NEWELL, D. R. (1984). *J. Med. Chem.* **27**, 870–874.

WILMAN, D. E. V. & GODDARD, P. M. (1991). *Prog. Pharmacol. Clin. Pharmacol.* **8**, 335–341.

Acta Cryst. (1992). B**48**, 217–227

Electrostatic Properties of 1-Methyluracil from Diffraction Data

BY W. T. KLOOSTER, S. SWAMINATHAN, R. NANNI AND B. M. CRAVEN

Department of Crystallography, University of Pittsburgh, Pittsburgh, Pennsylvania 15260, *USA*

(*Received* 24 *May* 1991; *accepted* 7 *November* 1991)

Abstract

1-Methyluracil (1-methyl-2,4-dioxopyrimidine), $C_5H_6N_2O_2$, $M_r = 126.12$, orthorhombic, *Ibam*, $a = 13.188\ (6)$, $b = 13.175\ (5)$, $c = 6.214\ (3)$ Å, $V = 1079.7\ (8)$ Å^3, $Z = 8$, $D_x = 1.552$ g cm^{-3}, λ(Mo $K\alpha$) $= 0.7107$ Å, $\mu = 1.317$ cm^{-1}, $F(000) = 528$, $T = 123$ K, $R(F^2) = 0.068$ for 2996 reflections with $\sin\theta/\lambda < 1.08$ Å^{-1}. The electronic charge-density distribution has been analyzed in terms of Stewart's rigid pseudoatom model, using restricted Slater radial functions and angular multipole terms extending to octapoles for C, N and O, and quadrupoles for H pseudoatoms. Three different structure refinements have been carried out based on two X-ray diffraction data sets from different crystals collected at temperatures differing by about 20 K. The molecular dipole moment is 6.4 (27) D. Maps of the electrostatic potential for a molecule isolated from the crystal show that atoms O2 and O4 confer overall electronegativity on one side of the molecule while the CH groups and the C1 methyl group confer electropositivity on the other. For the centrosymmetric hydrogen-bonded dimer (N3—H3···O4′; H···O distances 1.77 Å) the electrostatic potential shows electropositive bridges between the molecules. These features are lacking for the C—H···O interactions (distances H6···O2, 2.37; H11···O4, 2.34 Å). The electron density and its Laplacian have been determined at the intramolecular bond-critical points and also for the intermolecular H···O interactions. Values for the former are characteristic of covalent bonds. Values of the electron density and Laplacian for the C—H···O interactions are very small and have little

0108-7681/92/020217-11$03.00

© 1992 International Union of Crystallography

or no significance in terms of their e.s.d.'s. The electrostatic energy of interaction for the N—H···O hydrogen-bonded dimer is $-10\,(12)$ kJ mol^{-1}. The attractive electrostatic energy increases to $-67\,(33)$ kJ mol^{-1} for a centrosymmetric planar tetramer in which the C—H···O interactions are also formed.

Introduction

The nucleic acids are strongly polar molecules owing to the formal negative charge on each phosphate and to the polar groups both in the base and sugar residues. Thus electrostatic properties are important for understanding the stereochemistry and dynamical behavior of the nucleic acids. For this reason, X-ray and sometimes neutron diffraction have been used to determine the charge-density distribution in crystal structures of nucleic acid components, including uracil (Stewart, 1970), 9-methyladenine (Craven & Benci, 1981), cytosine monohydrate (Eisenstein, 1988; Weber & Craven, 1990) and ammonium dimethylphosphate (Klooster & Craven, 1992). Also, Pearlman & Kim (1990) have determined net atomic charges for cytidine, adenosine, deoxyadenosine, deoxythymidine, deoxycytidylic acid and guanylic acid. We now report a study of 1-methyluracil (Fig. 1) which was undertaken because this molecule is one of the bases occurring in RNA.

The crystal structure of 1-methyluracil at room temperature was first determined by Green, Mathews & Rich (1962). McMullan & Craven (1989; hereafter MC) have determined the structure from neutron diffraction data collected at 15, 60 and 123 K and carried out a thermal-vibrational analysis at each temperature. In the crystal structure of 1-methyluracil, the molecules are very efficiently packed to form sheets which lie in the crystallographic mirror planes $z = 0, \frac{1}{2}$ in the space group *Ibam*. As shown in Fig. 2, the molecules form hydrogen-bonded dimers N3—H3···O4 with symmetry 2/*m*. Atom O2 does not form hydrogen bonds of the usual kind, but both O2 and O4 are involved in close intermolecular interactions with C—H groups (H6···O2, 2.37; H11···O4, 2.34 Å). For further details of the molecular geometry and crystal packing, see MC and Green *et al.* (1962). Our study of the charge-density distribution is based on two X-ray (Mo $K\alpha$) data sets, one of which was collected close to 123 K and the other at a temperature about 20 K higher.

Experimental

Two X-ray data sets were collected on different crystals and independent structure refinements were carried out. The first data set was collected and the refinement was completed before the neutron data of MC were collected. After the neutron results became available, it appeared that the first X-ray study [henceforth (I)] was based on data collected with the crystal at a temperature somewhat higher than was used in the neutron study (123 K). The second X-ray study, (II), was undertaken with the aim of matching

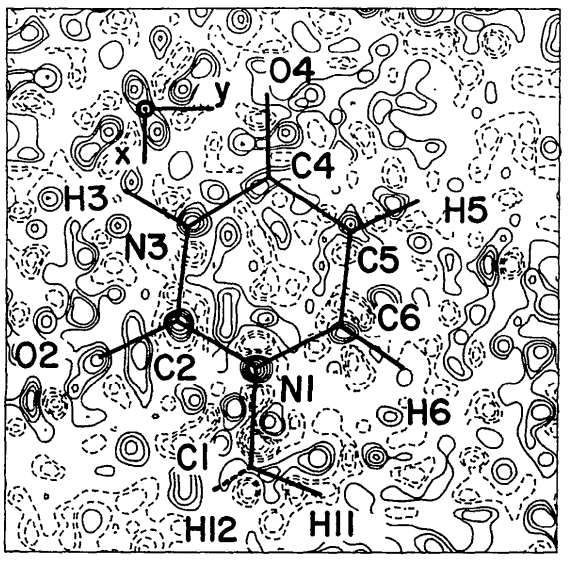

Fig. 1. Difference Fourier synthesis of residual density after refinement (IIv). The section is $z = 0$, which is a crystallographic mirror plane passing through all atoms except H12. Contours are at an interval of 0.06 e Å^{-1} which is equal to the estimated standard deviation in the electron density at the origin of the unit cell. The zero contour is not shown.

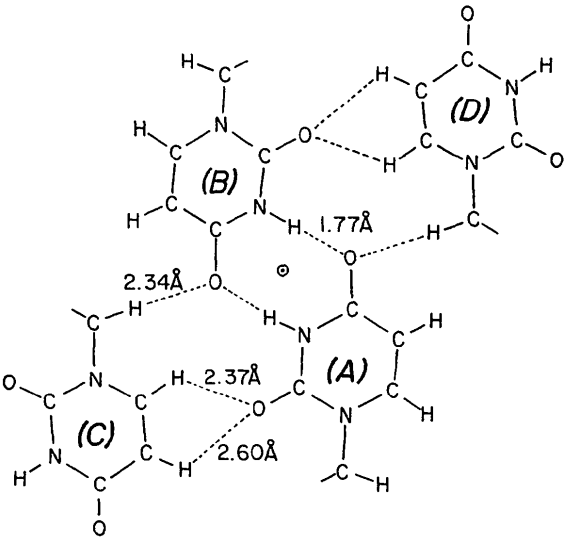

Fig. 2. A tetramer of 1-methyluracil molecules with point symmetry 2/*m* taken from the crystal structure. The short H···O distances from MC are shown by dashed lines. Molecules (*A*) and (*B*) form a doubly hydrogen-bonded dimer. Molecules (*C*) and (*D*) each make C—H···O interactions with (*A*) and (*B*).

Table 1. *Unit-cell parameters* (Å) *for* 1-*methyluracil*

The temperatures with subscripts refer to the thermocouple reading in the cold-stream bathing crystals (I) and (II).

	Neutron, MC 123 K	123 $K_{(I)}$	293 $K_{(I)}$	101 $K_{(II)}$	111 $K_{(II)}$	123 $K_{(II)}$	146 $K_{(II)}$
a	13.214 (2)	13.192 (3)	13.200 (2)	13.186 (5)	13.188 (6)	13.184 (6)	13.192 (4)
b	13.193 (3)	13.183 (2)	13.226 (2)	13.174 (4)	13.175 (5)	13.177 (5)	13.187 (4)
c	6.213 (1)	6.239 (1)	6.372 (2)	6.206 (2)	6.214 (3)	6.222 (2)	6.243 (2)

more closely the temperature of the neutron study. The experimental procedures for (I) and (II) were very similar. Unless specifically stated below, the details and results provided are for (II).

Crystals of 1-methyluracil (Chemical Dynamics Corp., NJ) were grown from aqueous ethanol by slow evaporation. The crystals were from the same sample as the larger crystals used by MC. X-ray diffraction data (Nb-filtered Mo $K\alpha$ radiation, λ = 0.71069 Å) were collected using a crystal with dimensions 0.28 × 0.28 × 0.38 mm which was elongated along the *c* axis and showed the forms {110} and {001}. The crystal was mounted with the *c* axis about 10° from the φ axis of an Enraf–Nonius CAD-4 diffractometer. The crystal was bathed in a stream of cold nitrogen gas with the temperature monitored by a thermocouple located 8 mm upstream. In order to minimize ice formation on the crystal, the diffractometer was placed in a sealed box filled with dried air.

The unit-cell dimensions at a given temperature were obtained from a least-squares fit of $\sin^2\theta$ values for 25 reflections in the range $18 < \theta < 24°$. Each reflection was measured at four equivalent positions (two with positive and two with negative θ) in order to correct for possible crystal mis-centering. Because of our concern that the temperature of the cold stream might not be the true crystal temperature, efforts were made to match the MC cell dimensions by making measurements over a range of cold-stream temperatures (Table 1). The *c* dimension is the most temperature sensitive, since this corresponds to the direction of stacking of molecular layers which interact weakly with each other in the crystal structure. Changes in *a* and *b* are smaller because these are the dimensions within the closely packed layers. Unfortunately, we could not obtain satisfactory agreement with MC values at any temperature in the range 101 to 146 K. We have no explanation for the systematic differences between the X-ray and neutron measurements which are most notable for *a* and *b*. However, using X-ray diffraction, there is agreement between the cell dimensions for crystal (I) and those determined for (II) at a cold-stream temperature of 146 K, indicating that the temperature of crystal (I) during data collection was probably at least 20 K higher than the intended 123 K. The intensity data for crystal (II) were collected at a cold-stream temperature of 111 K because this gave the best agreement with *c* as reported by MC.

X-ray intensities were measured by $\omega/2\theta$ scans, with ω-scan width $(0.50 + 0.35\tan\theta)°$, scan speed 0.80–1.33° min^{-1}. Data collection was for the octant of reciprocal space with $\sin\theta/\lambda < 1.08$ $Å^{-1}$ and with $h, k < 28, l < 13$. Integrated intensities were obtained using the method of Lehmann & Larsen (1974) for scan-profile analysis. For reflections with $\theta < 7°$ backgrounds were estimated using the method of Nelmes (1975). The intensities of five reflections ($\bar{1}0,7,1$, 10,7,1, 008, 0,0,10, 0,0,12) were monitored every 1500 s of data collection. There were no significant variations in the first two of these. The higher orders of 00*l* were useful for monitoring changes in the crystal temperature. The 00*l* intensities depend on the mean-square displacements of atoms perpendicular to the molecular layers and these displacements are temperature sensitive as shown by MC. Slow variations (~24 h) of as much as 20% were observed in the intensity of 0,0,12 ($\sin\theta/\lambda = 0.97$ $Å^{-1}$) corresponding to variations $\Delta U^{33} = 0.0008$ $Å^2$ for the mean-square atomic displacements. These indications of crystal-temperature variations necessitated the remeasurement of many reflections and the application of scaling factors as determined from variation of the 00*l* monitor reflections. An absorption correction ($\mu = 1.317$ cm^{-1}) was applied (Busing & Levy, 1957), which gave correction factors from 1.030 to 1.036. These calculations also provided mean crystal path lengths (0.25 to 0.30 mm) which were used for estimating extinction effects (see below). A total of 2996 independent reflections were measured, including 1696 reflections having $F^2 > 1.5\sigma(F^2)$.

The electronic charge-density distribution in the crystal structure was determined by full-matrix least-squares refinement based on the rigid-pseudoatom model of Stewart (1976). The pseudoatom cores were assumed to consist of neutral Hartree–Fock isolated atoms with X-ray scattering factors given by Cromer & Waber (1974). For H atoms, spherical bonded-atom X-ray scattering factors were assumed (Stewart, Davidson & Simpson, 1965). Pseudoatom deformation terms were assigned a Slater-type radial function with a fixed standard value for the radial exponent (α = 6.42, 7.37, 8.50, 4.69 $Å^{-1}$ for C, N, O

and H respectively; Hehre, Stewart & Pople, 1969). Angular functions were obtained from a multipole expansion about each pseudoatom nucleus. The expansion was up to the octapole level, but with constraints on the number of terms owing to the crystallographic mirror plane at $z = 0$ which passes through all nuclei except H12. A complete description of the pseudoatom X-ray scattering factors is given by Epstein, Ruble & Craven (1982). Refinements were carried out using earlier versions of computer programs by Craven, Weber & He (1987). The function $\sum w\Delta^2$ was minimized, where in the case of refinement with data set (II), $\Delta = |F_o^2| - |F_c^2|$ and $w = \sigma^{-2}(F_o^2)$, with $\sigma^2 = \sigma_{cs}^2 + (0.02F_o^2)^2$. All 2996 reflections were included. For refinement with data set (I), $\Delta = |F_o| - |F_c|$ and $w = \sigma^{-2}(F_o)$, and only those 1484 reflections were included for which $|F_o| > 3\sigma(F)$.

For refinement (I), initial atomic parameters were derived from Green *et al.* (1962) for the heavier atoms. Variables for each of these atoms consisted of the two positional parameters, four anisotropic displacement parameters and ten electron-population parameters. Fixed H-atom positions were taken from neutron diffraction results for 1-methylthymine (Kvick, Koetzle & Thomas, 1974). The variables refined for each H atom were an isotropic displacement parameter, and the monopole and dipole electron-population parameters. Refinement for data set (I) with a total of 163 variables converged giving $wR(F) = 0.033$, $R(F) = 0.046$, $S = 1.32$.*

For refinement (II), the initial parameters included fixed values for nuclear positions of all atoms and anisotropic displacements for H as determined by MC from neutron diffraction. The variables consisted of the anisotropic displacement parameters for the heavier atoms and the electron-population parameters as described above except for the addition of quadrupole deformation for the H atoms. Also included was an isotropic extinction parameter assuming a type-I crystal with Lorentzian mosaicity (Becker & Coppens, 1974). The refined values of the anisotropic displacement parameters for the heavier atoms were in good agreement with those of MC except for U^{33}. Subsequently, anisotropic displacement parameters for heavier atoms were given fixed MC values, except for the U^{33} which remained as variables. The refinement with a total of 134 variables converged with $R(F^2) = 0.072$, $wR(F^2) = 0.086$, $S = 1.239$ and $[\Delta(p)/\sigma(p)] < 0.01$ for all variables.

A second refinement was carried out with data set (II) using the same structure model as before except that the core for each of the heavier pseudoatoms was assumed to be the K shell with a fixed population of two electrons rather than a complete Hartree–Fock atom. The K-shell scattering factors for C, N and O were taken from Cromer & Waber (1974). Radial exponents $\alpha = 6.14$, 7.37, 8.31 and 4.35 Å^{-1} were used for C, N, O and H respectively, these being the values obtained in the initial refinement cycles and subsequently fixed. During this refinement, which we call (IIv), it was noted that O2 had an unusually large dipole deformation. Also, a difference Fourier showed a peak of 0.40 (6) e Å^{-3} close to O2 as the most significant feature. Refinement was continued with the positional and anisotropic displacements for O2 included as variables. Significant changes were observed only for O2 (3σ in x, -3σ in d_1 and 2σ in U^{33}) and the residual density peak was reduced to 0.20 (6) e Å^{-3}. Refinement (IIv) converged with $R(F^2) = 0.068$, $wR(F^2) = 0.084$, $S = 1.200$ and $[\Delta(p)/\sigma(p)] < 0.05$ for all 140 variables.* The final value for the extinction parameter was $g = 0.164\,(13)$ rad^{-1}. The largest extinction correction was 1.47 for $F^2(002)$ and the next largest was 1.07. A final difference Fourier synthesis (Fig. 1) showed the largest residual features to be peaks at the nuclear positions for the ring atoms. However, the largest [0.30 (9) e Å^{-3}] is no more than marginally significant. With the valence-shell model used in refinement (IIv), the sum of monopole population parameters (p_v) over the pseudoatoms of one molecule should ideally be the total number of valence-shell electrons (48 for 1-methyluracil). Since the unconstrained value obtained from the (IIv) refinement was $\sum p_v = 44.6$ (2) e, the final population parameters from refinement (IIv) (Table 2) have been scaled by the factor 1.076 so that they correspond to a neutral molecule.

In Table 3, values of U^{33} from refinements (I), (II) and (IIv) are listed together with those from MC. It can be seen that the mean-square displacements obtained from (I) are the largest and are significantly greater than the MC values for all atoms. These results are consistent with the conclusions drawn above, based on unit-cell dimensions, *i.e.* that data set (I) was collected at a higher temperature than that used for the neutron data. Data set (II) may also have been collected at a somewhat higher temperature. The differences are smaller but all values are greater than those of MC except for C6.

We believe that the data from crystals (I) and (II) are of similar quality. We prefer the results of refinement (IIv) over the others because refinement (I) was carried out with more variables per observa-

* $R = \sum|\Delta|/\sum|F_o^m|$; $wR = (\sum w\Delta^2/\sum w|F_o^m|^2)^{1/2}$; $S = [\sum w\Delta^2/(n_{obs} - n_{prm})]^{1/2}$ where $m = 1$ for refinement (I) and $m = 2$ for (II).

* A table of reflection data for refinement (IIv) has been deposited with the British Library Document Supply Centre as Supplementary Publication No. SUP 54681 (28 pp.). Copies may be obtained through The Technical Editor, International Union of Crystallography, 5 Abbey Square, Chester CH1 2HU, England.

Table 2. *Electron population parameters* ($\times 10^2$)

Pseudoatom deformations are as defined by Epstein *et al.* (1982) and are referred to the orthogonal crystal axes. The population parameters are normalized according to Hansen & Coppens (1978). Thus all except monopole values are divided by 4π compared with those defined by Epstein *et al.* (1982). The crystallographic mirror plane ($z = 0$) requires that $d_3 = q_3 = q_4 = o_3 = o_4 = o_7 = 0$ except for H12 [for H12 in refinement (IIv), $d_3 = 1.10\,(30)$, $q_3 = -1.49\,(33)$, $q_4 = 1.14\,(34)$]. For each atom, entries are for refinement (I) (above), (II) (middle) and (IIv) (below). Note that $-p_v$ is the net charge on each pseudoatom. For refinement (IIv), the values listed are $(p_v - n_v)$ where n_v is the number of valence-shell electrons and p_v is the observed number of valence-shell electrons.

	p_v	d_1	d_2	q_1	q_2	q_5	o_1	o_2	o_5	o_6
N1	−5 (5)	−44 (41)	−6 (35)	16 (37)	68 (39)	126 (44)	172 (33)	12 (33)	−116 (34)	−13 (31)
	6 (4)	96 (22)	−54 (19)	−11 (22)	−92 (23)	95 (23)	232 (30)	0 (31)	4 (29)	−65 (27)
	−5 (5)	117 (23)	−60 (21)	10 (24)	−76 (25)	157 (29)	223 (32)	0 (33)	−7 (30)	−67 (29)
N3	18 (5)	25 (41)	−44 (35)	−69 (37)	−27 (39)	−44 (39)	254 (31)	2 (33)	−3 (34)	−38 (31)
	11 (5)	52 (22)	−23 (23)	−1 (24)	40 (25)	79 (23)	257 (29)	−44 (34)	−17 (30)	38 (29)
	1 (6)	77 (24)	−10 (24)	3 (25)	10 (27)	150 (28)	239 (31)	−38 (35)	−20 (31)	32 (30)
C1	−4 (7)	135 (41)	−72 (44)	−27 (40)	−136 (40)	29 (48)	−335 (38)	−78 (33)	240 (44)	−47 (41)
	−5 (10)	201 (31)	−34 (36)	−158 (31)	17 (31)	60 (38)	−178 (38)	−63 (37)	145 (42)	−189 (40)
	−52 (12)	169 (36)	−58 (42)	−131 (34)	−3 (34)	167 (45)	−195 (43)	−50 (42)	169 (46)	−188 (43)
C2	24 (6)	104 (38)	−116 (41)	−139 (37)	−196 (41)	−300 (44)	−398 (40)	66 (42)	25 (38)	−3 (38)
	12 (5)	189 (24)	−134 (25)	−88 (25)	−134 (27)	−249 (26)	−385 (34)	−1 (37)	−21 (31)	16 (33)
	17 (7)	179 (28)	−72 (30)	−70 (29)	−113 (31)	−257 (33)	−338 (40)	−4 (42)	−13 (35)	−21 (37)
C4	4 (6)	−79 (41)	63 (31)	192 (37)	75 (39)	−266 (44)	−313 (40)	21 (45)	119 (34)	−41 (34)
	3 (5)	3 (25)	−21 (22)	84 (25)	41 (25)	−263 (26)	−325 (35)	56 (41)	−78 (31)	107 (31)
	−4 (7)	56 (31)	−46 (26)	68 (30)	63 (29)	−296 (33)	−305 (41)	56 (48)	−114 (35)	96 (34)
C5	18 (6)	57 (44)	−116 (35)	85 (40)	−45 (41)	−121 (44)	292 (40)	−120 (40)	−19 (41)	−19 (34)
	1 (6)	66 (29)	−46 (27)	41 (29)	−18 (29)	−93 (27)	292 (37)	−96 (41)	91 (36)	−4 (31)
	−9 (8)	95 (35)	−63 (32)	68 (34)	−47 (34)	−122 (34)	367 (43)	−120 (47)	88 (40)	−17 (34)
C6	3 (6)	−60 (44)	−82 (38)	24 (43)	−19 (40)	−184 (39)	−264 (38)	75 (38)	−106 (44)	19 (34)
	−6 (6)	47 (30)	76 (27)	52 (29)	30 (28)	−178 (26)	−286 (35)	84 (38)	−157 (38)	4 (30)
	−12 (9)	89 (36)	40 (32)	9 (34)	16 (33)	−229 (33)	−303 (40)	99 (44)	−180 (42)	11 (33)
O2	−3 (4)	104 (21)	−151 (41)	75 (40)	139 (41)	39 (53)	−33 (26)	17 (26)	−81 (34)	−34 (31)
	5 (3)	138 (17)	−158 (19)	132 (20)	50 (20)	53 (22)	−14 (24)	44 (25)	−42 (29)	33 (28)
	22 (4)	57 (32)	−92 (33)	79 (32)	52 (34)	82 (41)	−9 (24)	53 (26)	−53 (31)	16 (30)
O4	3 (4)	−75 (44)	−31 (31)	−45 (37)	12 (39)	−135 (44)	45 (26)	19 (28)	−3 (34)	34 (31)
	12 (3)	−74 (18)	4 (16)	−155 (19)	−48 (19)	−19 (20)	20 (25)	−1 (25)	−62 (29)	−9 (27)
	28 (4)	−33 (33)	14 (28)	−89 (31)	−36 (33)	106 (37)	41 (26)	6 (26)	−75 (30)	10 (28)
H3	−18 (4)	107 (35)	120 (38)	–	–	–	–	–	–	–
	−25 (4)	72 (31)	190 (35)	−67 (38)	174 (43)	−48 (40)				
	−14 (4)	118 (35)	237 (39)	−83 (42)	202 (48)	−104 (44)				
H5	−11 (3)	145 (31)	−138 (35)	–	–	–	–	–	–	–
	−7 (4)	109 (34)	−159 (38)	−39 (44)	−119 (47)	−29 (44)				
	−1 (5)	155 (39)	−212 (45)	−28 (49)	−124 (52)	−81 (49)				
H6	−10 (4)	−82 (35)	−267 (38)	–	–	–	–	–	–	–
	−6 (4)	−71 (31)	−139 (35)	13 (42)	−21 (48)	−157 (45)				
	5 (5)	−106 (36)	−182 (41)	12 (48)	−18 (54)	−209 (50)				
H11	2 (5)	−160 (44)	−283 (47)	–	–	–	–	–	–	–
	−15 (5)	−31 (36)	−189 (43)	−147 (44)	55 (47)	93 (55)				
	1 (4)	−124 (41)	−349 (50)	−205 (49)	156 (53)	6 (61)				
H12	−25 (6)	−305 (41)	164 (41)							
	6 (3)	−33 (24)	74 (26)	189 (26)	−42 (27)	−45 (40)				
	13 (4)	−76 (27)	110 (30)	48 (28)	−39 (29)	13 (45)				

tions than was the case for (II) and (IIv),* and because the agreement factors and goodness-of-fit for (IIv) were a little better than for (II).

* Unfortunately, the data for crystal (I) are no longer available in computer-readable form. Thus we have not carried out a refinement based on F_o^2, including all reflections, as was done for (II) and (IIv).

Discussion

A comparison of electron-population parameters from refinements (I), (II) and (IIv) (Table 2) shows general agreement although there are some differences, which mostly involve the values obtained in refinement (I). The most significant differences in terms of the estimated errors include d_1 (3.4σ) and q_2

Table 3. *Anisotropic displacement parameters, U^{33}* ($Å^2 \times 10^4$)

The parameter U^{33} which determines the mean-square atomic displacement from the molecular plane ($z = 0$) is defined by the expression $T = \exp(-2\pi^2\sum_i\sum_j h_i h_j a^{*i} a^{*j} U_{ij})$. Columns (I), (II) and (IIv) give present results from refinements based on X-ray diffraction data. Column MC gives results of McMullan & Craven (1989) based on neutron diffraction data collected at 123 K.

	(I)	(II)	(IIv)	MC
N1	207 (7)	201 (5)	184 (4)	187 (3)
C2	203 (7)	176 (5)	181 (4)	166 (4)
N3	227 (7)	204 (5)	191 (4)	184 (3)
C4	192 (6)	174 (5)	181 (4)	151 (4)
C5	237 (8)	211 (6)	223 (5)	187 (4)
C6	196 (7)	168 (5)	180 (4)	182 (4)
C1	389 (10)	418 (9)	387 (7)	354 (5)
O2	331 (9)	317 (6)	301 (7)	268 (5)
O4	294 (7)	277 (5)	248 (6)	236 (5)

(3.1σ) for N1, q_5 (4.0σ) for N3, and o_5 (4.8σ) for C4. It must be remembered that the data used for refinement (I) came from a different crystal and that the data were probably collected at a higher temperature (by about 20 K). Also, neutron diffraction data were not available for (I). It is of interest that the dipole populations for the H atoms in (I) agree reasonably well with (II) and (IIv). This indicates that reliable H-atom positional parameters were derived for (I) by assuming the neutron diffraction results for 1-methylthymine (Kvick *et al.*, 1974). The most significant differences involving monopole populations occur for C1 and H12. In (IIv), there is a depletion in charge at C1 which is much greater than in (I) and (II). This is the largest effect attributable to the difference in the model used for the charge distribution in refinement (IIv). However, the net charge $-\sum p_v$ for the four atoms of the methyl group (C1, H11, H12 and H12′) is +0.52 (12), +0.08 (12) and +0.25 (14) in (I), (II) and (IIv) respectively. Thus, the methyl group is electropositive in each case and only the partitioning of charge is different. In difference Fourier syntheses, the residual density in the region of the methyl group is not helpful in distinguishing the two models. The negative trough of −0.25 (7) e $Å^{-3}$ near C1 in Fig. 1 corresponds to a peak of 0.20 (5) e $Å^{-3}$ obtained for the other model.

As might be expected from comparison of the population parameters, there are similarities in the deformation-density maps obtained for (I), (II) and (IIv) (Fig. 3). These maps are for pseudoatoms at rest, calculated by summing the pseudoatom deformation-density functions given by Epstein *et al.* (1982). The greatest differences in the deformation density are in the C4—O4 and N1—C1 bonds. These can be attributed to the differences already noted in the population parameters for these atoms. At O4, non-bonding density consistent with lone-pair features is present in the plane of the ring (Fig. 3),

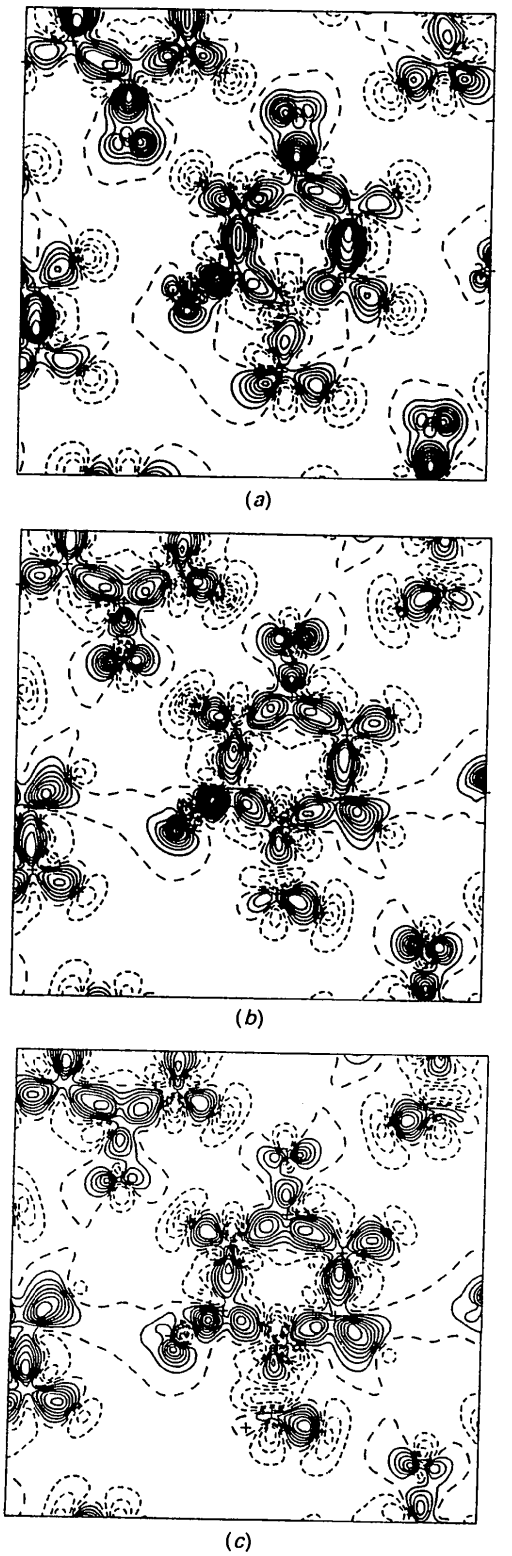

(*a*)

(*b*)

(*c*)

Fig. 3. The deformation charge density for 1-methyluracil in the section $z = 0$ calculated with the atoms at rest. Contours are at intervals of 0.1 e $Å^{-3}$. (*a*) Refinement (I). (*b*) Refinement (II). (*c*) Refinement (IIv).

but at O2 these features are developed in an unusual way. As can be seen in Fig. 4, the deformation density almost encircles O2 in the plane normal to the C2—O2 bond. These effects at O2 may be real since they are observed in (I), (II) and (IIv). However, lone-pair density features are generally unreliable because it is difficult to deconvolute them from the effects of thermal vibration of the O atom. They are described by quadrupole deformations which have the same symmetry as the components of the anisotropic atomic displacement.

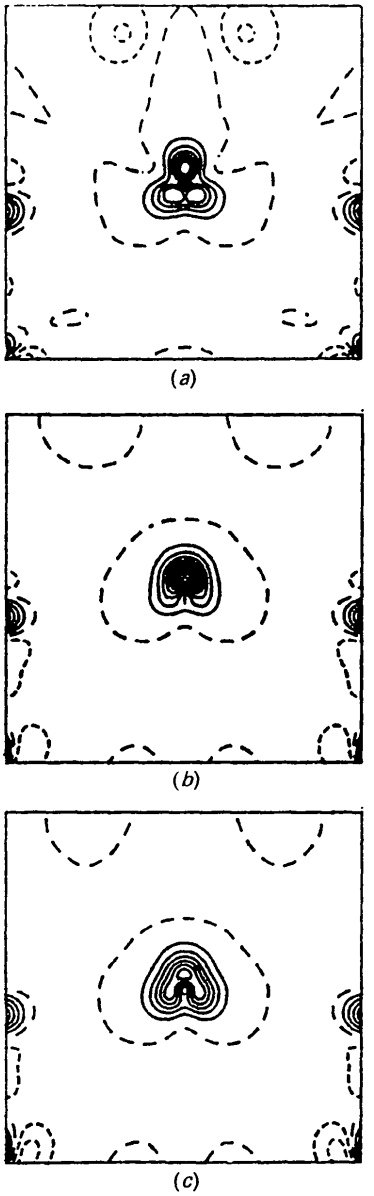

Fig. 4. The deformation charge density as in Fig. 3, but for a section showing the density surrounding O2. This section is normal to the C2—O2 bond at a distance of 0.1 Å from O2. (*a*) Refinement (I). (*b*) Refinement (II). (*c*) Refinement (IIv).

In Fig. 5, we show the Laplacian of the electron density $\nabla^2\rho(r)$ in the section of the mirror plane through the molecule. In this calculation, $\rho(r)$ is the total electron density for pseudoatoms at rest as obtained from refinement (IIv).* As has been pointed out by Bader & Essén (1984), the negative regions of the Laplacian (those above the zero plane in Fig. 5) correspond to local concentrations of electron density and positive regions are local depletions. Thus the Laplacian is negative at the nuclear positions and in regions corresponding to the positive deformation density in Fig. 3, including the nonbonding density at O2 and O4. The strong oscillations shown in Fig. 5 close to the C, N and O nuclei are caused by the *K*-shell structure in the electron density.

The Laplacian is of particular interest at the saddle point in $\rho(r)$ which occurs between each pair of bonded atoms (Bader & Essén, 1984). At these so-called bond-critical points (listed in Table 4 for 1-methyluracil), the gradient in $\rho(r)$ is zero. The Laplacian can be written $\nabla^2\rho(r) = \lambda_1 + \lambda_2 + \lambda_3$,

* Calculations involving the Laplacian (Fig. 5 and Table 4) made use of an updated version of the *VALRAY* computer program package (Stewart & Spackman, 1983). As a preliminary, the least-squares refinement with model (IIv) was repeated. The resulting population parameters were in very close agreement with those in Table 2 which were obtained with the *POP* programs (Craven, Weber & He, 1987).

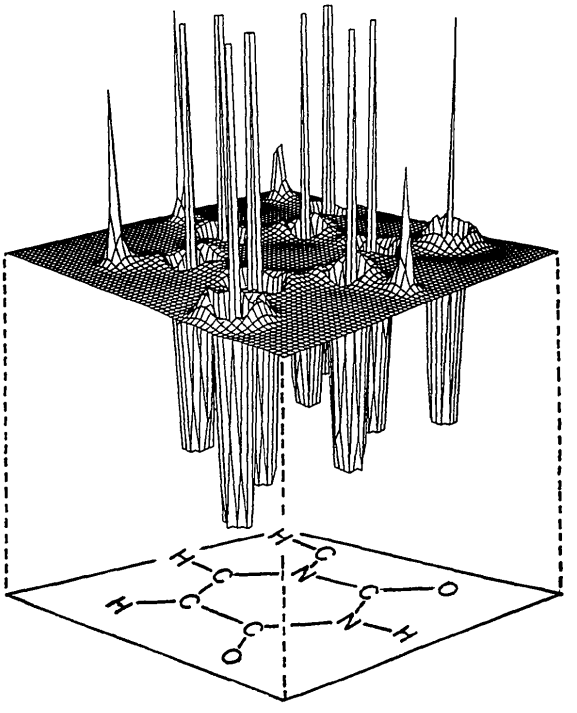

Fig. 5. The negative Laplacian of the total electron density (atoms at rest) for 1-methyluracil. This plot is for the section through the ring atoms. The Laplacian is zero in the central plane with negative values plotted above the plane.

Table 4. *Bond-critical-point data*

For each critical point, the first line gives values (e.s.d.'s in parentheses) for the total charge density calculated for a static arrangement of pseudoatoms with parameters from refinement (IIv). The second line gives values for the corresponding arrangement of neutral spherical Hartree–Fock atoms. Bond distances (d, Å) are those obtained by MC from neutron diffraction at 123 K, and (x,y) are fractional coordinates in the unit cell for the bond-critical point. The z coordinate is zero for all bond-critical points except C1—H12, where $z = 0.0951$ (first line) and 0.0966 (second line). The electron density $\rho(r)$ is in e Å^{-3} and the Laplacian $\nabla^2\rho(r) = \lambda_1 + \lambda_2 + \lambda_3$, where λ_k are the principle values of the curvature, is in e Å^{-5}. For all critical points except C6—H6 and C1—H12, λ_2 is in the direction perpendicular to the molecular plane.

(*a*) Intramolecular bonds

	d	x	y	$\rho(r)$	$\nabla^2\rho(r)$	λ_1	λ_2	λ_3
N1—C1	1.459	0.3558	0.1210	1.46 (7)	−5.6 (27)	−9.4	−7.9	11.7
		0.3469	0.1233	1.47	2.2	−7.4	−7.2	16.9
N1—C2	1.380	0.2567	0.0778	2.19 (7)	−16.7 (24)	−18.5	−14.5	16.3
		0.2558	0.0761	1.68	−1.3	−8.7	−8.3	15.7
N1—C6	1.367	0.2586	0.1796	2.29 (8)	−22.7 (27)	−19.6	−17.9	14.8
		0.2587	0.1794	1.72	−2.1	−8.9	−8.6	15.3
N3—C2	1.377	0.1915	0.0412	2.13 (7)	−19.7 (24)	−18.6	−15.1	13.9
		0.1880	0.0416	1.69	−1.5	−8.7	−8.4	15.6
N3—C4	1.384	0.0990	0.0972	2.27 (7)	−19.7 (24)	−18.5	−17.4	16.2
		0.0983	0.0981	1.67	−1.1	−8.6	−8.3	15.8
C4—C5	1.441	0.1071	0.1841	2.01 (8)	−18.5 (23)	−16.3	−12.9	10.8
		0.1056	0.1820	1.38	−0.9	−6.5	−6.2	11.8
C5—C6	1.354	0.1918	0.2225	2.19 (7)	−20.8 (24)	−19.3	−11.2	9.8
		0.1872	0.2229	1.59	−4.2	−7.6	−7.4	10.8
C2—O2	1.225	0.2508	0.0043	3.00 (7)	−29.0 (39)	−28.6	−23.8	23.4
		0.2476	0.0079	2.14	7.1	−11.6	−11.3	30.1
C4—O4	1.238	0.0395	0.1359	2.70 (9)	−20.6 (39)	−26.7	−21.9	28.0
		0.0416	0.1363	2.11	5.1	−11.3	−11.1	27.5
N3—H3	1.040	0.0983	−0.0037	2.15 (9)	−36.7 (45)	−31.6	−29.3	24.2
		0.0988	−0.0033	1.48	−6.4	−15.4	−15.3	24.3
C5—H5	1.080	0.1144	0.2752	2.00 (6)	−25.00 (25)	−20.3	−18.3	13.6
		0.1124	0.2781	1.24	−4.6	−9.6	−9.5	14.4
C6—H6	1.088	0.2715	0.2627	2.05 (8)	−23.2 (25)	−21.4	−19.0	17.3
		0.2714	0.2643	1.23	−4.3	−9.4	−9.3	14.3
C1—H11	1.079	0.4147	0.1662	2.02 (7)	−25.1 (28)	−20.0	−16.2	11.0
		0.4170	0.1724	1.25	−4.6	−9.6	−9.5	14.5
C1—H12	1.080	0.4113	0.0951	2.00 (6)	−19.5 (23)	−19.0	−17.6	17.0
		0.4136	0.0923	1.25	−4.6	−9.5	−9.5	14.6

(*b*) Intermolecular interactions

These are identified in Fig. 2. For the interactions H5···O2 (distance 2.60 Å), the search for a bond-critical point was unsuccessful.

H3···O4	1.77	0.0617	−0.0598	0.23 (3)	2.1 (8)	−1.9	−1.7	5.7
		0.0616	−0.0639	0.31	3.0	−1.6	−1.6	6.1
H6···O2	2.37	0.2490	0.3573	0.07 (2)	1.1 (1)	−0.4	−0.3	1.9
		0.2550	0.3573	0.09	1.1	−0.3	−0.3	1.7
H11···O4	2.34	0.4487	0.2651	0.06 (8)	0.6 (25)	−0.4	−0.3	1.3
		0.4522	0.2675	0.10	1.1	−0.3	−0.3	1.8

where the λ_k are the three principal values of the curvature in $\rho(r)$. The λ_k are eigenvalues of the Hessian matrix with elements $\partial^2\rho/\partial x_i\partial x_j$ and are associated with mutually orthogonal directions. At a bond-critical point, one principal curvature (λ_3) is positive because $\rho(r)$ increases along the path towards both bonded atoms. The remaining two (λ_1, λ_2) are negative because $\rho(r)$ is decreasing in other directions. In Table 4, the experimental values for the Laplacian of 1-methyluracil at the bond-critical points are compared with those for the corresponding superposition of noninteracting neutral spherical atoms. For the covalent bonds (Table 4*a*), the experimental values are all significantly more negative. This is because covalent bonding enhances the electron density along the path between the bonded atoms, tending to decrease the magnitude of λ_3 and increase the magnitude of $(\lambda_1 + \lambda_2)$. In Table 4(*a*), it can be seen that the experimental electron density and its Laplacian at the bond-critical points have similar values for bonds of the same type (C—N, C—O, C—C, C—H). However, values for the exocyclic C1—N1 bond (1.459 Å) involving the tetrahedral carbon are significantly smaller than those for the four ring C—N bonds (1.367 to 1.384 Å). According to simple valence-bond theory, C5—C6 (1.354 Å) has strong double-bond character while C4—C5 (1.441 Å) is better described as single. For the C=C bond-critical point in ethylene, Bader & Essén (1984) used a 6-31G* wavefunction to obtain $\rho(r) = 2.45$ e Å^{-3}, $\nabla^2\rho(r) = -28.65$ e Å^{-5} and λ values -19.63, -13.58, $+4.55$ e Å^{-5}. Corresponding values for the C—C bond in ethane are 1.70 e Å^{-3}, -15.94 and -11.50, -11.50, $+7.06$ e Å^{-5}. Comparison with the values in Table 4(*a*) indicate that the C—C bonds in 1-methyluracil

are of intermediate type with C5—C6 more like C=C in ethylene and C4—C5 more like C—C in ethane, but the experimental differences are small in terms of their e.s.d.'s. It is also interesting to compare bond ellipticities, defined as $\varepsilon = (\lambda_1 - \lambda_2)/\lambda_2$ evaluated at the bond-critical point. For σ-type bonds, such as the C—C bond of ethane, $\varepsilon = 0$ and for bonds with increasing π character, ε also increases. Thus for C=C in ethylene, $\varepsilon = 0.45$. In 1-methyluracil, $\varepsilon = 0.7$ (2) for C5—C6 and 0.3 (2) for C4—C5. None of the other bonds listed in Table 4(*a*) have ellipticities exceeding 0.3.

The molecular dipole moment was calculated from the monopole and dipole population parameters and the radial exponents, following the procedure of Stewart (1972). In order to determine $\sigma(\mu)$, the origin was chosen at the molecular center of mass. The magnitudes [$|\mu| = 10.4$ (24), 4.4 (22) and 6.4 (27) D with parameters from (I), (II) and (IIv) respectively] and the directions for these dipole moments are shown in Fig. 6. The results from (II) and (IIv) are in good agreement, as might be expected from the agreement in the corresponding atomic parameters. The greatest difference [between (I) and (II)] may be significant since $|\mu_{(I)} - \mu_{(II)}|$ differs from zero by 3.2σ. The dipole moments for 1-methyluracil obtained from (II) and (IIv) are very similar to the value of $|\mu| = 4.0$ (13) D reported by Stewart (1970) from an *L*-shell projection study of the crystal structure of uracil. The general conclusion from these estimates of the dipole moment is that the region of the carbonyl groups is electronegative and the region of the CH and CH_3 groups is electropositive.

This effect is shown in greater detail in the map of electrostatic potential for the molecule isolated from the crystal structure (Fig. 7). Our calculation of the potential is based on a procedure developed by Stewart (1983) and summarized by He (1984). The most electronegative feature shown in Fig. 7 is the minimum close to O2 (-0.244 e Å^{-1} or -339 kJ mol^{-1}), the minimum at O4 being shallower (-160 kJ mol^{-1}). These are opposite a diffuse region of positive potential extending from C5 to the C1 methyl group. In the plane 1 Å distant from the molecular mirror plane, the potential is electropositive except for the region above O2. The electronegative minima near the O atoms in 1-methyluracil are intermediate in magnitude between those observed near the carbonyl O atoms in parabanic acid (-92 kJ mol^{-1}; He, Swaminathan, Craven & McMullan, 1988) and for the O atom in urea (-440 kJ mol^{-1}). The latter value was obtained by Stewart (1983) from data reported by Swaminathan, Craven, Spackman & Stewart (1984). As might be expected, the electronegativity of the O atoms tends to increase with increasing C—O bond length (1.206, 1.214 and 1.215 Å in parabanic acid; 1.227 and 1.241 Å in 1-methyluracil; 1.264 Å in urea). The map of electrostatic potential for an isolated thymine molecule based on *ab initio* molecular orbital calculations by Bonaccorsi, Pullman, Scrocco & Tomasi (1972) agrees qualitatively with

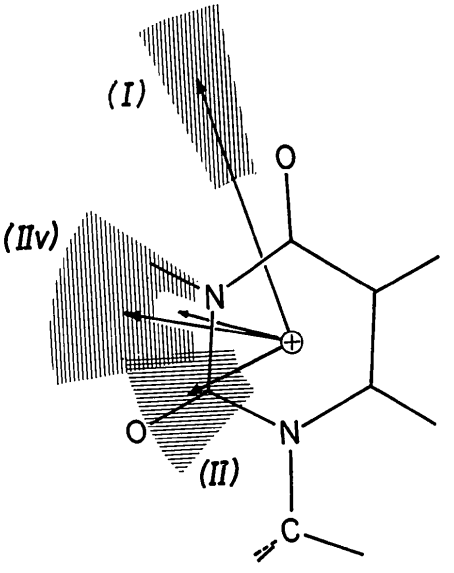

Fig. 6. The dipole moments for 1-methyluracil obtained from refinements (I), (II) and (IIv) with magnitudes $|\mu| = 10.4$, 4.4 and 6.4 D respectively. The shaded area for each represents $\pm\sigma$ in the magnitude and direction of μ. The unlabeled arrow (near N3) represents the dipole moment for uracil (Stewart, 1970).

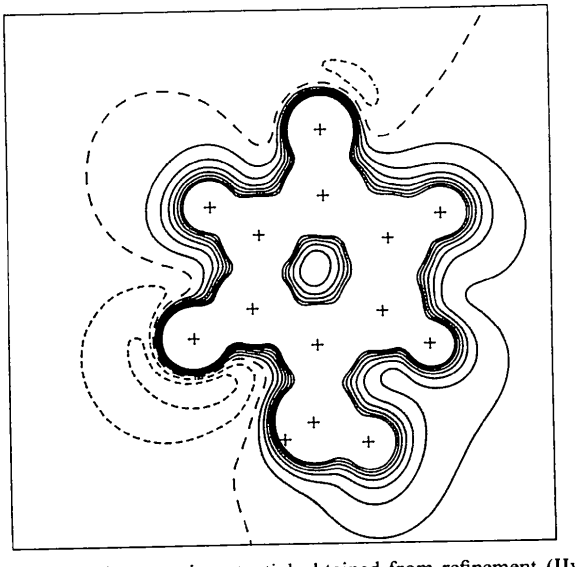

Fig. 7. The electrostatic potential obtained from refinement (IIv) for a molecule of 1-methyluracil isolated from the crystal structure. The section is in the plane of the ring atoms. Contours are at an interval of 0.1 e Å^{-1} with dashed contours for regions of electronegativity.

Fig. 7. Their map shows minima of −210 and −236 kJ mol^{-1} at O2 and O4 respectively.

In the crystal structure of 1-methyluracil the electrostatic interactions of the molecules are of special interest because, in addition to the conventional N—H···O hydrogen bonding, there are short C—H···O distances (Fig. 2). In Fig. 8 we show the electrostatic potential around the center of a cluster of 15 molecules taken from the plane $z = 0$ in the crystal structure. As was seen in similar maps for phosphorylethanolamine (Swaminathan & Craven, 1984), parabanic acid (He *et al.*, 1988) and the complex of parabanic acid with thiourea (Weber & Craven, 1987) there are low bridges of electropositivity connecting molecules in the H···O region of the N—H···O hydrogen bonds. Although the magnitude of the electropositive potential is cluster-size dependent, the existence of a bridge appears to be a characteristic of normal hydrogen bonds. However, such a feature is absent in the H···O regions of the C—H···O interactions in Fig. 8, so that by this criterion, the C—H···O interactions are not hydrogen bonds.

We have considered whether the electron density and its Laplacian at the bond-critical points might provide useful criteria for comparing the N—H···O and C—H···O interactions. As can be seen from Table 4(*b*), the critical points were located for the N—H···O hydrogen bond and for two of the C—H···O interactions. However, for the third of the interactions shown in Fig. 2 (H5···O2; 2.60 Å), the search procedure was not convergent. The electron density in this region was very small and was effectively uniform. For the N—H···O hydrogen bond, the electron density at the H···O critical point is 0.23 (3) Å^{-3} which is significantly nonzero although somewhat smaller than the density obtained from the independent-atom model (0.31 e Å^{-3}). The observed Laplacian has a small positive value 2.1 (8) e Å^{-5}, this being consistent with an interaction between closed-shell atoms or ions. For the two C—H···O interactions, the electron density is only marginally if at all nonzero at the critical points and the values of the Laplacian are very small and not significantly different from the corresponding values obtained from the independent-atom model. We conclude that this approach does not provide support for the occurrence of H···O bonding in the C—H···O interactions of 1-methyluracil.

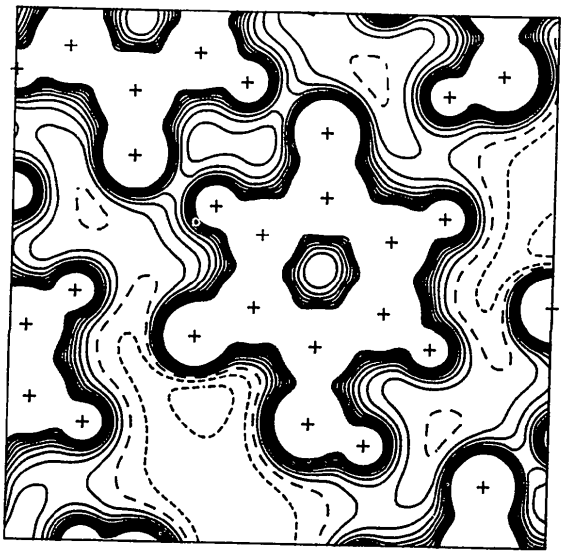

Fig. 8. The electrostatic potential as in Fig. 7 but for the central region of a cluster of 15 nearest neighbor molecules all in the plane $z = 0$.

Spackman (1986) has developed a point-multipole model for calculating the interaction energy of hydrogen-bonded molecules and this has been applied by Spackman, Weber & Craven (1988) to several hydrogen-bonded crystal structures. With this procedure, we find for the hydrogen-bonded dimer consisting of molecules *A* and *B* in Fig. 2 that the electrostatic energy of interaction is −10 (12) kJ mol^{-1}. This is small when compared with the energy −50 (14) kJ mol^{-1} obtained by Spackman *et al.* (1988) for the head-to-tail doubly hydrogen-bonded dimer in urea. It is interesting that the addition of molecule *C* (Fig. 2) gives an electrostatic interaction energy of −38 (25) kJ mol^{-1} for the trimer. This enhancement of the attractive interaction is achieved by introducing a molecule which forms short C—H···O intermolecular distances with both molecules of the *AB* dimer. We see that the electropositive side of molecule *C* has been brought against the electronegative side of the *AB* dimer. For the centrosymmetric planar tetramer (*ABCD*) the electrostatic energy of interaction is further increased to −67 (33) kJ mol^{-1}. We would not characterize the individual C—H···O interactions as hydrogen bonds, for the reasons given above. However, the collective effect of bringing the electropositive regions of molecules *C* and *D* close to the electronegative regions of the *AB* dimer has provided stability for the tetramer which outweighs the contribution of the conventional N—H···O hydrogen bonds.

The crystal structure of uracil (Stewart & Jensen, 1967) is very similar to that of 1-methyluracil. It has a layer structure with N3—H3···O4 hydrogen-bonded dimers and has two C—H···O interactions with short H···O distances of 2.32 and 2.42 Å. Other short distances have been observed in the crystal structures of ribonucleotides. Thus in the nonhelical structure of the dinucleotide UpA containing two independent molecules, Sussman, Seeman, Kim & Berman (1972) report that in each molecule there is an intramolecular C···O distance (3.14, 3.18 Å)

involving C6 of uracil and O5′ of the uridine ribose. It seems likely that the short C—H···O distances in these different crystal environments arise as a result of electrostatic attractions very similar to those which we presently describe for 1-methyluracil.

We thank Dr Robert F. Stewart for calculation of the bond-critical point data (Table 4 and Fig. 5) and for his critical reading of the manuscript. We also thank Dr John R. Ruble and Mrs J. Klinger for technical assistance. This work was supported by grant GM-39513 from the National Institutes of Health.

References

BADER, R. F. W. & ESSÉN, H. (1984). *J. Chem. Phys.* **84**, 1943–1960.
BECKER, P. J. & COPPENS, P. (1974). *Acta Cryst.* A**30**, 129–147.
BONACCORSI, R., PULLMAN, A., SCROCCO, E. & TOMASI, J. (1972). *Theor. Chim. Acta (Berlin)*, **24**, 51–60.
BUSING, W. R. & LEVY, H. A. (1957). *Acta Cryst.* **10**, 180–182.
CRAVEN, B. M. & BENCI, P. (1981). *Acta Cryst.* B**37**, 1584–1591.
CRAVEN, B. M., WEBER, H. P. & HE, X. M. (1987). *The POP Least-Squares Refinement Procedure.* Tech. Rep. Department of Crystallography, Univ. of Pittsburgh, USA.
CROMER, D. T. & WABER, J. T. (1974). *International Tables for X-ray Crystallography*, Vol. IV, pp. 71–147. Birmingham: Kynoch Press. (Present distributor Kluwer Academic Publishers, Dordrecht.)
EISENSTEIN, M. (1988). *Acta Cryst.* B**44**, 412–426.
EPSTEIN, J., RUBLE, J. R. & CRAVEN, B. M. (1982). *Acta Cryst.* B**38**, 140–149.
GREEN, D. W., MATHEWS, F. S. & RICH, A. (1962). *J. Biol. Chem.* **273**, PC3573–3575.
HANSEN, N. K. & COPPENS, P. (1978). *Acta Cryst.* A**34**, 909–921.
HE, X. M. (1984). PhD Dissertation, Univ. of Pittsburgh, PA, USA.
HE, X. M., SWAMINATHAN, S., CRAVEN, B. M. & MCMULLAN, R. K. (1988). *Acta Cryst.* B**44**, 271–281.
HEHRE, W. J., STEWART, R. F. & POPLE, J. A. (1969). *J. Chem. Phys.* **51**, 2657–2664.
KLOOSTER, W. T. & CRAVEN, B. M. (1992). *Biopolymers.* In the press.
KVICK, Å., KOETZLE, T. F. & THOMAS, R. (1974). *J. Chem. Phys.* **61**, 2711–2717.
LEHMANN, M. S. & LARSEN, F. K. (1974). *Acta Cryst.* A**30**, 580–584.
MCMULLAN, R. K. & CRAVEN, B. M. (1989). *Acta Cryst.* B**45**, 270–276.
NELMES, R. J. (1975). *Acta Cryst.* A**31**, 273–279.
PEARLMAN, D. A. & KIM, S.-H. (1990). *J. Mol. Biol.* **211**, 171–187.
SPACKMAN, M. A. (1986). *J. Chem. Phys.* **85**, 6587–6601.
SPACKMAN, M. A., WEBER, H. P. & CRAVEN, B. M. (1988). *J. Am. Chem. Soc.* **110**, 775–782.
STEWART, R. F. (1970). *J. Chem. Phys.* **53**, 205–213.
STEWART, R. F. (1972). *J. Chem. Phys.* **57**, 1664–1668.
STEWART, R. F. (1976). *Acta Cryst.* A**32**, 565–574.
STEWART, R. F. (1983). Unpublished.
STEWART, R. F., DAVIDSON, E. R. & SIMPSON, W. T. (1965). *J. Chem. Phys.* **42**, 3175–3187.
STEWART, R. F. & JENSEN, L. H. (1967). *Acta Cryst.* **23**, 1102–1105.
STEWART, R. F. & SPACKMAN, M. A. (1983). *Valray User's Manual.* Department of Chemistry, Carnegie-Mellon Univ. Pittsburgh, PA, USA.
SUSSMAN, J. L., SEEMAN, N. C., KIM, S.-H. & BERMAN, H. M. (1972). *J. Mol. Biol.* **66**, 403–422.
SWAMINATHAN, S. & CRAVEN, B. M. (1984). *Acta Cryst.* B**40**, 511–518.
SWAMINATHAN, S., CRAVEN, B. M., SPACKMAN, M. A. & STEWART, R. F. (1984). *Acta Cryst.* B**40**, 398–404.
WEBER, H.-P. & CRAVEN, B. M. (1987). *Acta Cryst.* B**43**, 202–209.
WEBER, H.-P. & CRAVEN, B. M. (1990). *Acta Cryst.* B**46**, 532–538.

Acta Cryst. (1992). B**48**, 227–230

Structure of the Bromohydrin of an Octahydronaphthalene Derivative

BY G. D. FALLON, B. M. GATEHOUSE,* S. MIDDLETON AND S. P. VANNI

Chemistry Department, Monash University, Clayton, Victoria 3168, *Australia*

(*Received* 21 *August* 1991; *accepted* 20 *November* 1991)

Abstract

(±)-3β-Bromo-2β-methyl-4aβH,8aαH-decahydronaphthalen-2α-ol, $C_{11}H_{19}BrO$, $M_r = 247.2$, tetragonal, $I\bar{4}$, $a = 14.146$ (6), $c = 11.910$ (8) Å, $V = 2383$ (2) Å^3, $Z = 8$, $D_m = 1.37$ (2), $D_x = 1.38$ Mg m^{-3}, λ(Mo $K\alpha$) = 0.71073 Å, $\mu = 3.38$ mm^{-1}, $F(000) = 1024$, $T = 213$ K, final $R = 0.043$ for 705 counter reflections. The *trans*-fused six-membered rings are chair-shaped but somewhat flattened. The torsion angle O—C(2)—C(3)—Br is −169.1 (6)°, the departure from 180° being almost entirely due to lateral displacement of the bromine atom.

Introduction

A mixture of the stereoisomeric octahydronaphthalenes (1) and (2) was obtained by use of a simple three-step reaction sequence (LaLonde & Tobias, 1963). Treatment of the liquid mixture of hydrocarbons with *N*-bromosuccinimide in aqueous

* Author to whom correspondence should be addressed.

0108-7681/92/020227-04$03.00

© 1992 International Union of Crystallography